Atomistic Long-Term Simulation of Heat and Mass Transport

M. Ortiz (Caltech)

PIRE Workshop

University of Warwick, UK

September 15, 2014

The spatial and temporal gaps

- The essential difficulty: *Multiple scales*
  - *Atomic level rate-limiting processes: Thermal activation, transport, defects, grain boundaries…*
  - *But macroscopic processes of interest:*
    - *Mechanical properties at moderate strain rates*
    - *Long-term transport phenomena: Heat, mass…*
    - *Full chemistry: Corrosion, combustion…*
- *Time-scale gap*: From molecular dynamics (femtosecond) to macroscopic (seconds-years)
- *Spatial-scale gap*: From lattice defects (Angstroms) to macroscopic (mm-m)
- Problem intractable by brute force (even with exascale computing ☺), *ergo* must think…

Example: Material properties

10^{10} s^{-1}, 100 nm

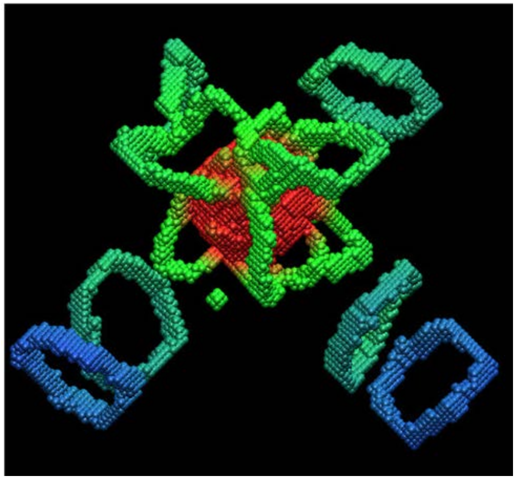

MD simulation of nanovoids growth in Ta[1]

10^{3} s^{-1}, 1 cm

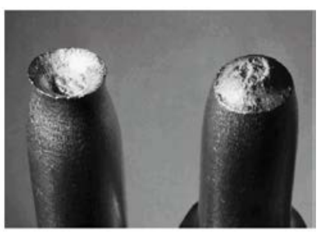

Cup-cone ductile fracture

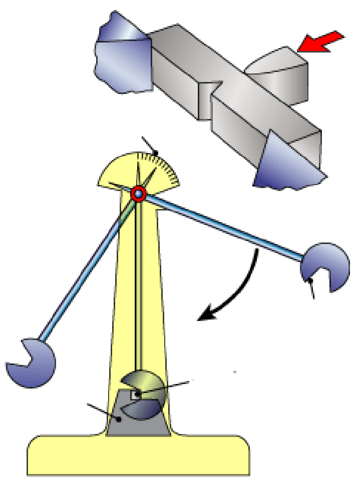

Charpy test

- Many mechanical properties are rate-controlled by lattice defects
- MD can access strain rates ~ 10^{8}-10^{12} s^{-1}, nano-samples
- Engineering applications involve lower strain rates, larger sizes
- Materials testing:
  - *Servo-hydraulic: 1* s^{-1}
  - *Hopkinson bar:* 10^{4} s^{-1}
  - *Plate impact:* 10^{7} s^{-1} *a*
- MD outside realm of typical engineering application and materials testing…

[1]Tang, Y., Bringa, E.M., Remington, B.A., and Meyers, M.A., *Acta Materialia*, **59**:1354, 2011

Example: Heat transport in Si nanowires

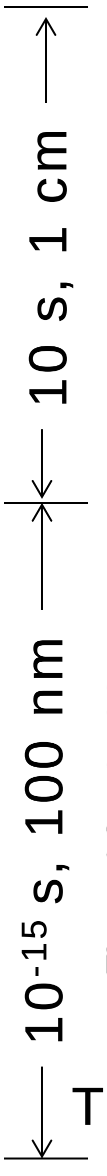

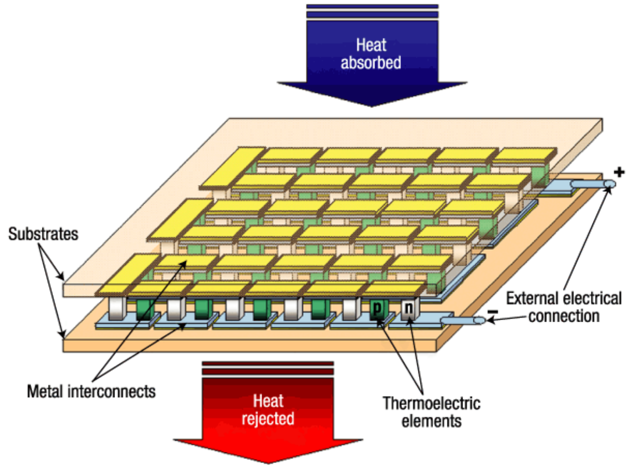

Thermoelectric device[1]

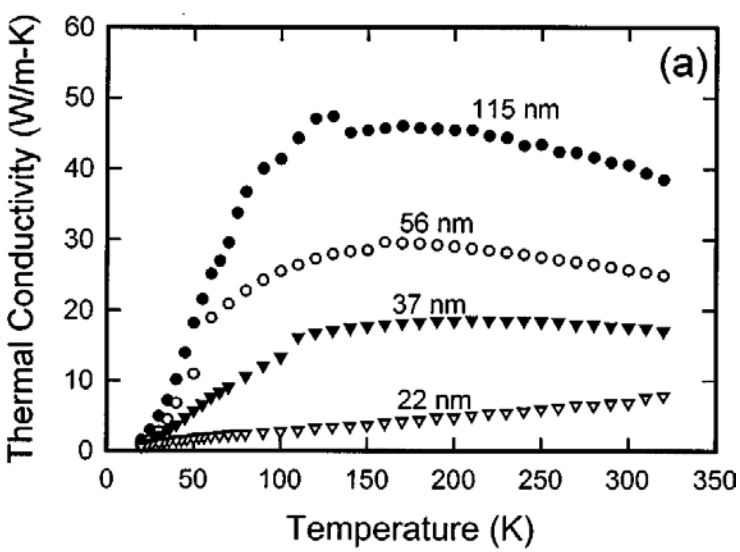

Thermal conductivity of Si NW[1]

- The thermal conductivity of NW exhibits size dependence not predicted by continuum models
- Low thermal conductivity yields high thermoelectric *ZT* values
- Typical devices are on the mm scale with thermal transients in the second time scale
- Outside range of straight MD...
- Also MD is often thermostated, which introduces artifacts

[1]G.J. Snyder, J.R. Lim, C.K. Huang and J.P. Fleurial, *Nature Materials.*,**2** (2003) 528.

[2]D. Li, Y. Yu, P. Kim, L. Shi, P. Yang and A. Majumdar, *Appl. Phys. Let.*,**83** (2003) 2934.

Example: Hydrogen storage

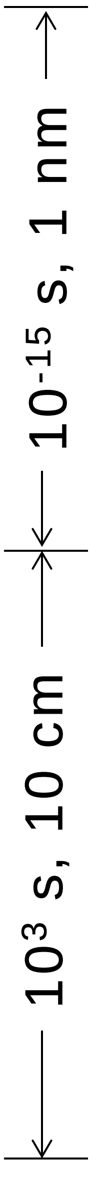

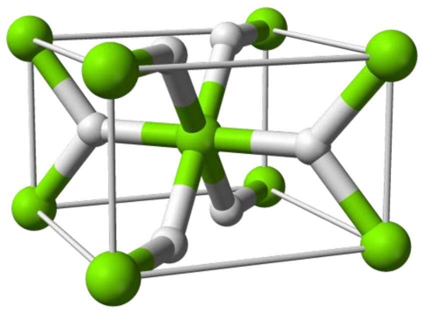

MgH_2 unit cell[1]

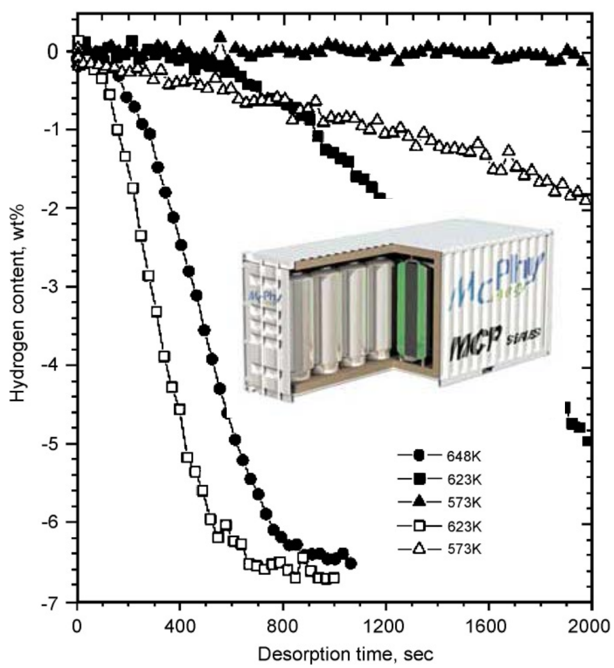

MgH_2 desorption curves[2]

- Metal hydrides (e.g. MgH_2) used for hydrogen storage, e.g., for use in fuel cells
- Absorption/desorption rates controlled at atomic level
- Commercial storage tanks have Kg capacities (McPhy Energy)
- Typical absorption/desorption times are temperature/pressure dependent and in hour range
- Outside range of straight MD...

[1]W. H. Zachariasen, C. E. Holley and J. F. Stamper, *J. Acta Cryst*, **16** (5):352-353.

[2]B. Sakintuna, F. Darkrim and M. Hirscher, *Int.J. Hydrogen Energy*, **32** (2007) 1121– 1140.

Example: Energetic materials

10^{-15} s, 1 nm

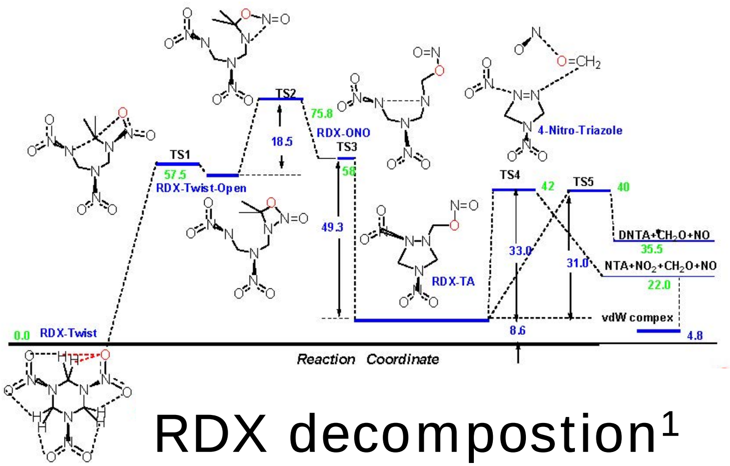

RDX decompostion[1]

10^{3} s, 10 m

Space Shuttle Atlantis[2]

- Energetic materials undergo complex chemistry coupled to temperature and deformation
- Reactions take place at atomic scale, involve bond breaking and creation of new bonds
- Reaction paths are extremely complex, defy reduce modeling
- Full chemistry, reaction-front speeds on the order of seconds
- Outside scope of straight MD...

[1]R. Asatryan, G. da Silva, J.W. Bozzelli (2008), 20th Intern. Symp. on Gas-Kinetics, Manchester, UK.

[2]http://www1.nasa.gov/images/

Spacetime atomistic-to-continuum

- ***Objectives***: Thermodynamics without all the thermal vibrations; mass transport without all the hops; atomistics without all the atoms…
- Our approach[1,2] (max-ent+kinetics+QC):
  - *Treat atomic-level fluctuations statistically by recourse to the* ***principle of maximum-entropy***
  - *Approximate grand-canonical free entropy using* ***variational meanfield theory***
  - *Append Onsager-like* ***empirical atomic-level kinetic laws*** *(heat and mass transport)*
  - *Treat (smooth)* ***mesodynamics*** *by implicit integration (large time steps >> MD!)*
  - ***Quasicontinuum*** *spatial coarse-graining*

[1]Y. Kulkarni, J. Knap & MO, *J. Mech. Phys. Solids*, **56** (2008) 1417.
[2]G. Venturini, K. Wang, I. Romero, M.P. Ariza & MO, *J. Mech. Phys. Solids*, (2014) in press.

Max-Ent Non-Equilibrium SM

- Grand-canonical ensemble, N atoms, M species:
  - State: $(\{\boldsymbol{q}\}, \{\boldsymbol{p}\}, \{\boldsymbol{n}\}) \in \mathbb{R}^{3N} \times \mathbb{R}^{3N} \times \mathcal{O}_{NM}$
  - Atomic positions: $\{\boldsymbol{q}\} = \{\boldsymbol{q}_1, \dots, \boldsymbol{q}_N\}$
  - Atomic momenta: $\{\boldsymbol{p}\} = \{\boldsymbol{p}_1, \dots, \boldsymbol{p}_N\}$
  - Occupancy: $n_{ik} = \begin{cases} 1, & \text{site } i \text{ occupied by species } k, \\ 0, & \text{otherwise.} \end{cases}$

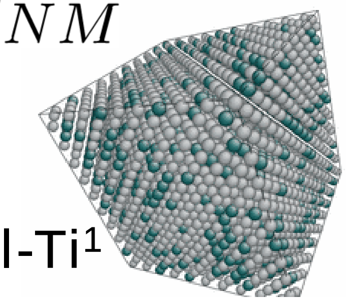
Al-Ti[1]

- Ensemble average of observable: $\langle A \rangle =$

$$\sum_{\{\boldsymbol{n}\} \in \mathcal{O}_{NM}} \int A(\{\boldsymbol{q}\}, \{\boldsymbol{p}\}, \{\boldsymbol{n}\}) \, \rho(\{\boldsymbol{q}\}, \{\boldsymbol{p}\}, \{\boldsymbol{n}\}) \, dq \, dp$$

↑ grand-canonical pdf

[1] J. von Pezold, A. Dick, M. Friak and J. Negebauer, Phys. Rev. B, 81 (2010) 094203.

Max-Ent Non-Equilibrium SM

- Assume $H = \sum_{i=1}^{N} h_i$, (e. g., EAM, TB...)
- Principle of max-ent[1]: $\mathcal{S}[p] = -k_B \langle \log \rho \rangle \to$ max!

subject to: $\langle \boldsymbol{q}_i \rangle = \bar{\boldsymbol{q}}_i,\ \langle \boldsymbol{p}_i \rangle = \bar{\boldsymbol{p}}_i,$
$\langle h_i \rangle = e_i,\ \langle n_{ik} \rangle = x_{ik}$ } local constraints!

- Lagrangian: reciprocal temperatures (β), chemical potentials (γ)

$$\mathcal{L}[p, \{\beta\}, \{\boldsymbol{\gamma}\}] = \mathcal{S}[p] - k_B \{\beta\}^T \{\langle h \rangle\} - k_B \{\boldsymbol{\gamma}\}^T \{\langle \boldsymbol{n} \rangle\}$$

- Gran-canonical pdf: $\rho = \frac{1}{\Xi} \mathrm{e}^{-\{\beta\}^T\{h\} - \{\boldsymbol{\gamma}\}^T\{\boldsymbol{n}\}},$

on affine subspace $\Big\{ \langle \{\boldsymbol{q}\} \rangle = \{\bar{\boldsymbol{q}}\}, \langle \{\boldsymbol{p}\} \rangle = \{\bar{\boldsymbol{p}}\} \Big\}$

[1]E.T. Jaynes, *Physical Review Series* II, **106**(4) (1957) 620–630; **108**(2) (1957) 171–190.

Max-Ent Non-Equilibrium SM

- Gran-canonical free entropy:

$$\Phi(\{\bar{\boldsymbol{q}}\},\{\bar{\boldsymbol{p}}\},\{\beta\},\{\gamma\}) = \underline{k_B \log \Xi}$$

- Mesoscopic Hamilton's equations:

$$\beta_i \frac{d\bar{\boldsymbol{q}}_i}{dt} = \frac{1}{k_B}\frac{\partial \Phi}{\partial \bar{\boldsymbol{p}}_i}, \quad \beta_i \frac{d\bar{\boldsymbol{p}}_i}{dt} = -\frac{1}{k_B}\frac{\partial \Phi}{\partial \bar{\boldsymbol{q}}_i}$$

- Local equilibrium relations:

$$e_i = -\frac{1}{k_B}\frac{\partial \Phi}{\partial \beta_i}, \quad x_{ik} = \frac{1}{k_B}\frac{\partial \Phi}{\partial \gamma_{ik}}$$

- Equilibrium SM recovered when $\beta_i = \beta$, $\gamma_{ik} = \gamma_k$
- **Essential difficulty:** Φ unknown, uncomputable

Non-equilibrium SM – Meanfield theory

- Space of trial *local Hamiltonians*: $\mathcal{H}_0$
- Free-entropy inequality: For all $\{h_0\} \in \mathcal{H}_0$,

  i) $\Phi \geq \Phi_0 - k_B \{\beta\}^T \{\langle h - h_0 \rangle_0\} \equiv \mathcal{S}[\{h_0\}]$

  ii) $\Phi = \mathcal{S}[\{h_0\}] \Leftrightarrow \{h_0\} = \{h\}$

- Best approximation: $\Phi_{\text{MF}} = \max_{\{h_0\} \in \mathcal{H}_0} \mathcal{S}[\{h_0\}]$
- Meanfield mesoscopic dynamics:

$$\beta_i \frac{d\bar{\boldsymbol{q}}_i}{dt} = \frac{1}{k_B} \frac{\partial \Phi_{\text{MF}}}{\partial \bar{\boldsymbol{p}}_i}, \quad \beta_i \frac{d\bar{\boldsymbol{p}}_i}{dt} = -\frac{1}{k_B} \frac{\partial \Phi_{\text{MF}}}{\partial \bar{\boldsymbol{q}}_i}$$

- Meanfield local equilibrium relations:

$$e_i = -\frac{1}{k_B} \frac{\partial \Phi_{\text{MF}}}{\partial \beta_i}, \quad x_{ik} = \frac{1}{k_B} \frac{\partial \Phi_{\text{MF}}}{\partial \gamma_{ik}}$$

Non-equilibrium SM – Meanfield theory

- Example: $\mathcal{H}_0 \equiv$ local harmonic oscillators,

$$h_{0i} = \frac{1}{2m(\boldsymbol{n}_i)}|\boldsymbol{p}_i - \bar{\boldsymbol{p}}_i|^2 + \frac{m(\boldsymbol{n}_i)\omega_i^2}{2}|\boldsymbol{q}_i - \bar{\boldsymbol{q}}_i|^2$$

- Entropy function (parameterized by $\{\omega\}$):

$$\mathcal{S}(\{\bar{\boldsymbol{q}}\}, \{\bar{\boldsymbol{p}}\}, \{\beta\}, \{\gamma\}, \{\omega\}) = \Phi_0 - k_B\{\beta\}^T\{\langle h - h_0\rangle_0\}$$

- Meanfield mesoscopic dynamics:

$$\beta_i \frac{d\bar{\boldsymbol{q}}_i}{dt} = \frac{1}{k_B}\frac{\partial \mathcal{S}}{\partial \bar{\boldsymbol{p}}_i}, \quad \beta_i \frac{d\bar{\boldsymbol{p}}_i}{dt} = -\frac{1}{k_B}\frac{\partial \mathcal{S}}{\partial \bar{\boldsymbol{q}}_i}, \quad \frac{\partial \mathcal{S}}{\partial \omega_i} = 0$$

- Meanfield local equilibrium relations:

$$e_i = -\frac{1}{k_B}\frac{\partial \mathcal{S}}{\partial \beta_i}, \quad x_{ik} = \frac{1}{k_B}\frac{\partial \mathcal{S}}{\partial \gamma_{ik}}$$

Non-equilibrium SM – Meanfield theory

- Example: $\mathcal{H}_0 \equiv$ local harmonic oscillators,

$$h_{0i} = \frac{1}{2m(\boldsymbol{n}_i)}|\boldsymbol{p}_i - \bar{\boldsymbol{p}}_i|^2 + \frac{m(\boldsymbol{n}_i)\omega_i^2}{2}|\boldsymbol{q}_i - \bar{\boldsymbol{q}}_i|^2$$

- Entropy function (parameterized by $\{\omega\}$):

$$\mathcal{S} = \sum_{i=1}^{N} k_B \left(\frac{\beta_i}{2m_i}|\bar{\boldsymbol{p}}_i|^2 + \beta_i \langle V_i \rangle_0 + 3\log(\hbar\beta_i\omega_i) - 3 \right)$$

Gaussian integrals!
Hermite quadrature!

- Meanfield mesoscopic dynamics:

$$\dot{\bar{\boldsymbol{q}}}_i = \frac{\bar{\boldsymbol{p}}_i}{m_i}, \quad \dot{\bar{\boldsymbol{p}}}_i = -\frac{\partial}{\partial \bar{\boldsymbol{q}}_i} \sum_{j=1}^{N} \langle V_j \rangle_0,$$

- Meanfield optimality: $\frac{\partial}{\partial \omega_i} \sum_{j=1}^{N} \beta_j \langle V_j \rangle_0 + \frac{3}{\omega_i} = 0$

Non-equilibrium SM – Meanfield validation

Binary EAM potential by: R. Johnson, *Phys. Rev. B*, **39**(17):12554, 1989

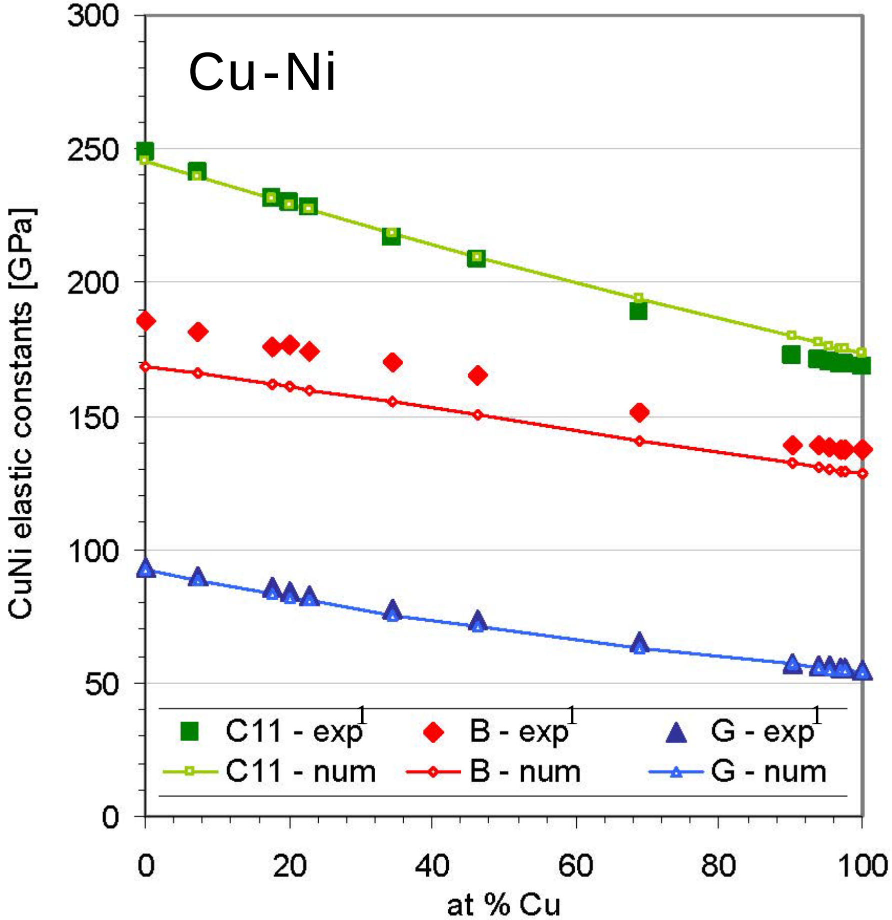

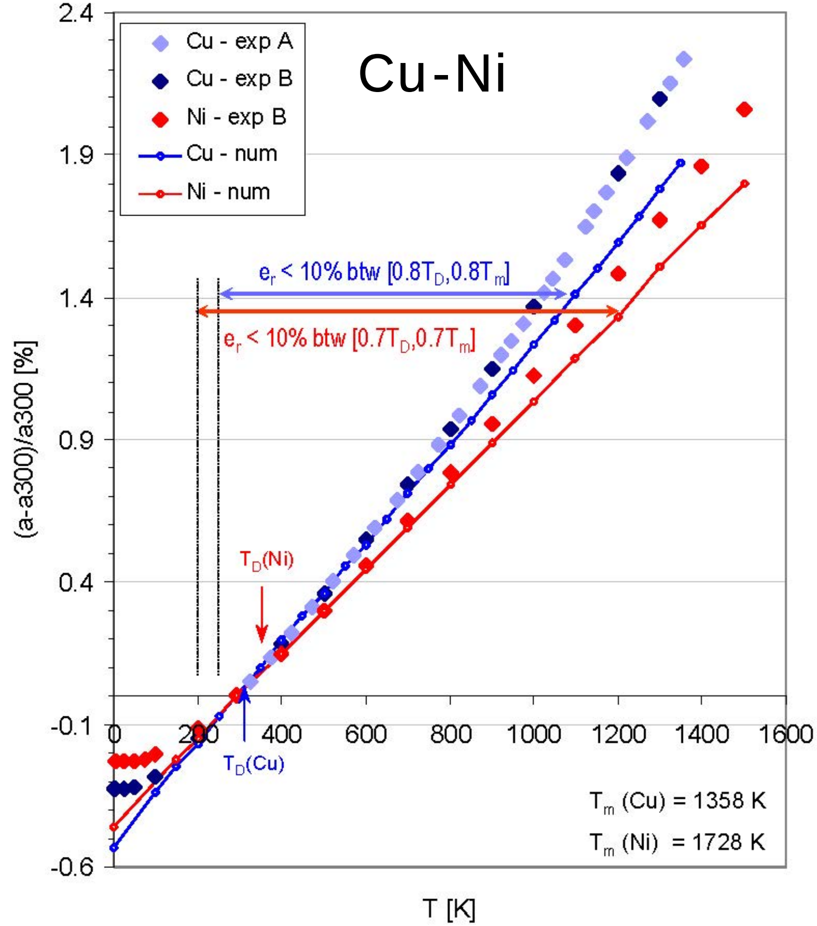

[1]Simmons, G., The MIT Press (1971).

[A]R. Simmons and R., Balluffi, *Phys. Rev.*, **129** (1963) 1533.

[B]R. Toloukian, The TPRC Data Series, vol. 12, 1975.

Michael Ortiz
PIRE 09/14

Non-equilibrium SM – Meanfield validation

Binary EAM potential by: R. Johnson, *Phys. Rev. B*, **39**(17):12554, 1989

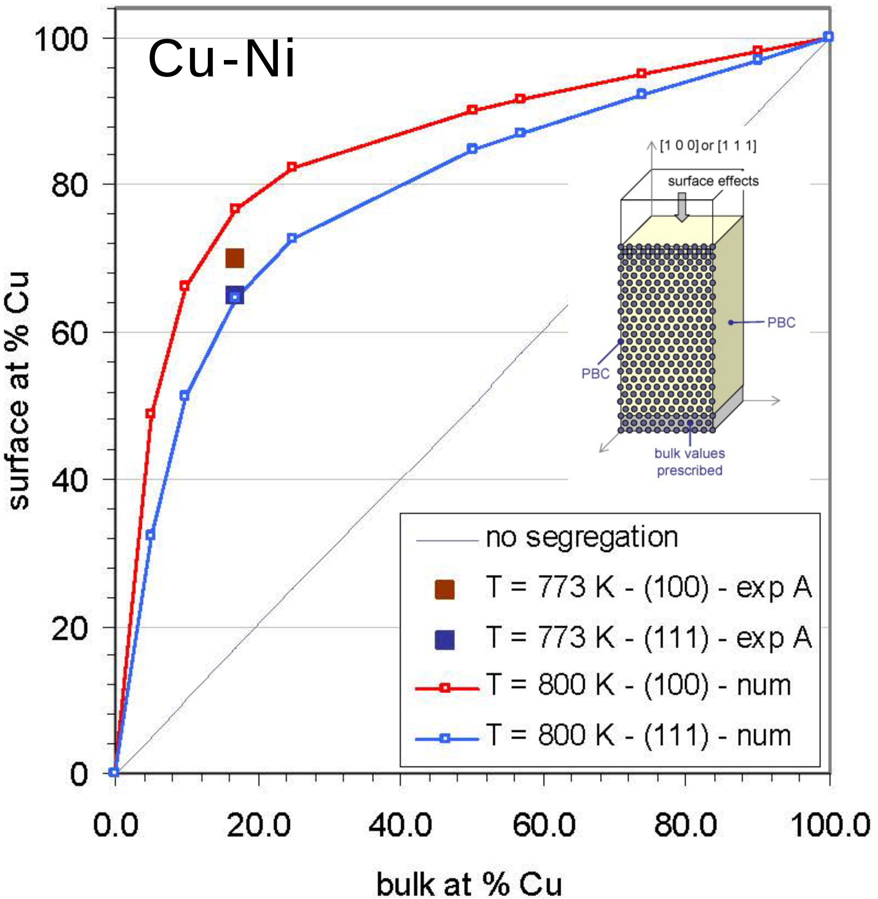

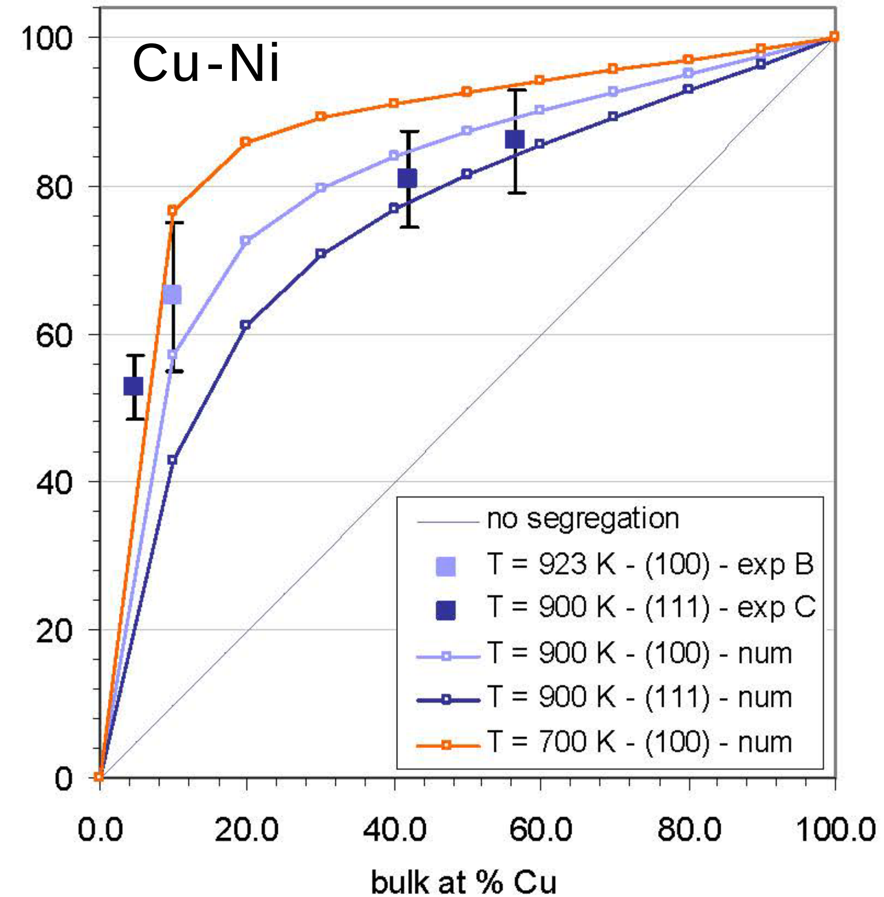

[A]K. Wandelt and C., Brundle, *Phys. Rev. Lett.*, **46** (1981) 1529–1532.
[B]C. Helms and K. Yu, *J. Vac. Sci. Technol.*, **12** (1975) 276–278.
[C]T. Sakurai, T. Hashizume and A. Sakai, A., *PRL*, **55** (1985) 514–517.

Non-equilibrium SM – Meanfield validation

Binary EAM potential by: R. Johnson, *Phys. Rev. B*, **39**(17):12554, 1989

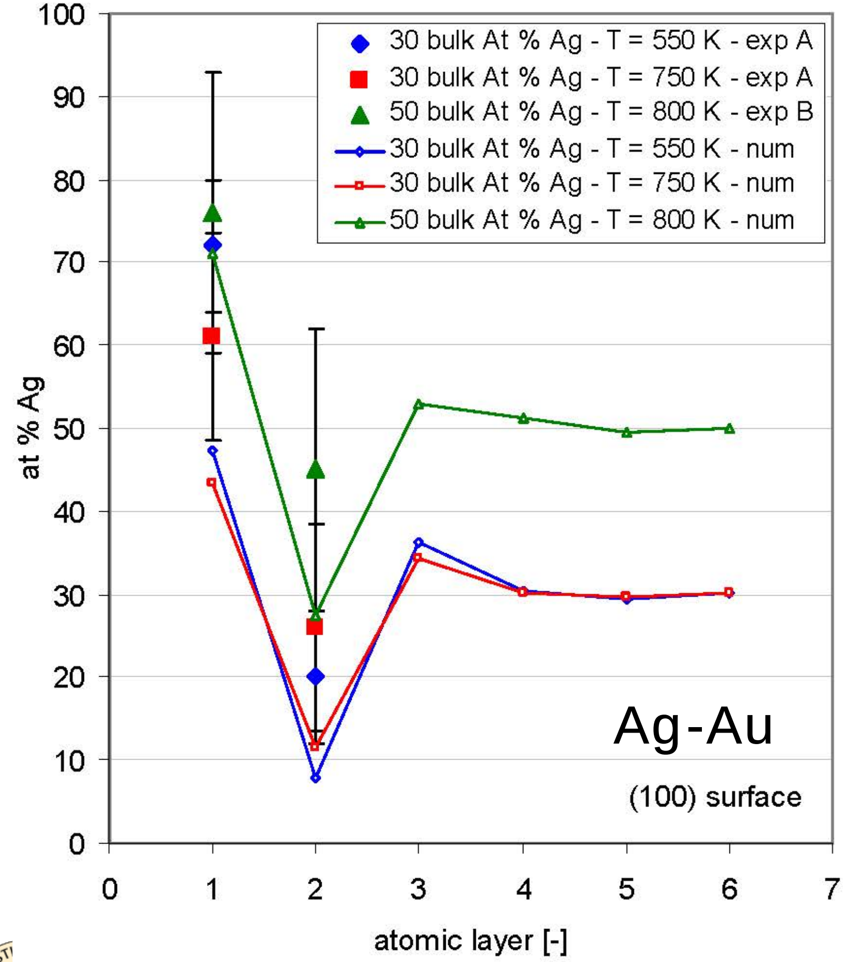

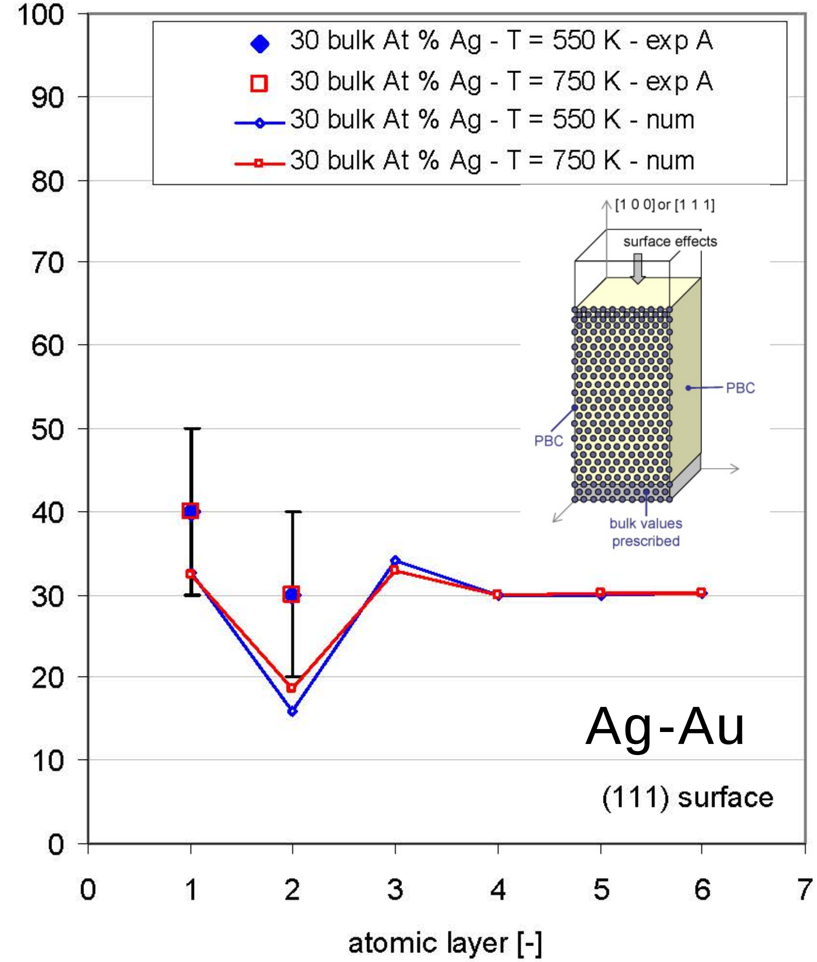

[A] T. King and R. Donnelly, *Surf. Sci.*, **151** (1985) 374–399.
[B] C. Derry, G., Wan, R., *Surf. Sci.*, **566-568** (2004) 862–868.

Non-equilibrium SM – Kinetics

- Need equations of evolution for $\{\beta\}$ and $\{\gamma\}$
- Local conservation equations:

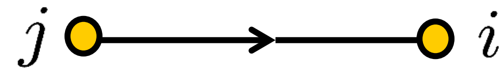

$$\underbrace{\dot{e}_i = \dot{w}_i + \boldsymbol{\mu}_i^T \dot{\boldsymbol{x}}_i + \sum_{j \neq i} R_{ij},}_{\text{energy}} \quad \underbrace{\dot{\boldsymbol{x}}_i = \sum_{j \neq i} \boldsymbol{J}_{ij}}_{\text{mass}}$$

- Local dissipation inequality:

$$\Sigma_{ij} = k_B(\beta_i - \beta_j) R_{ij} + k_B(\boldsymbol{\gamma}_i - \boldsymbol{\gamma}_j) \cdot \boldsymbol{J}_{ij} \geq 0$$

- General kinetic relations: calibrate from exp. data!

$$\underbrace{R_{ij} = f(\beta_i - \beta_j),}_{\text{Discrete Fourier law}} \quad \underbrace{\boldsymbol{J}_{ij} = g(\boldsymbol{\gamma}_i - \boldsymbol{\gamma}_j)}_{\text{Discrete Fick's law}}$$

Kinetic validation – Si nanowires

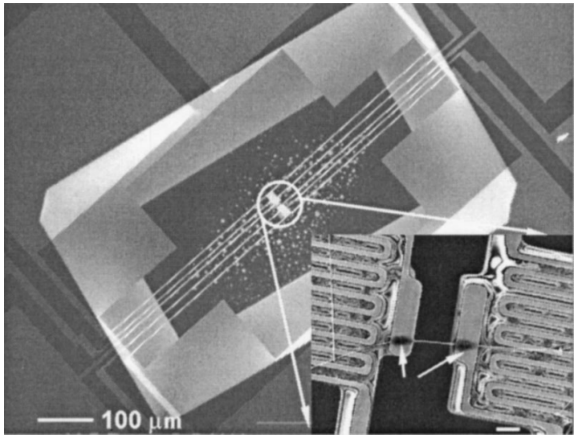

Experimental rig[1]

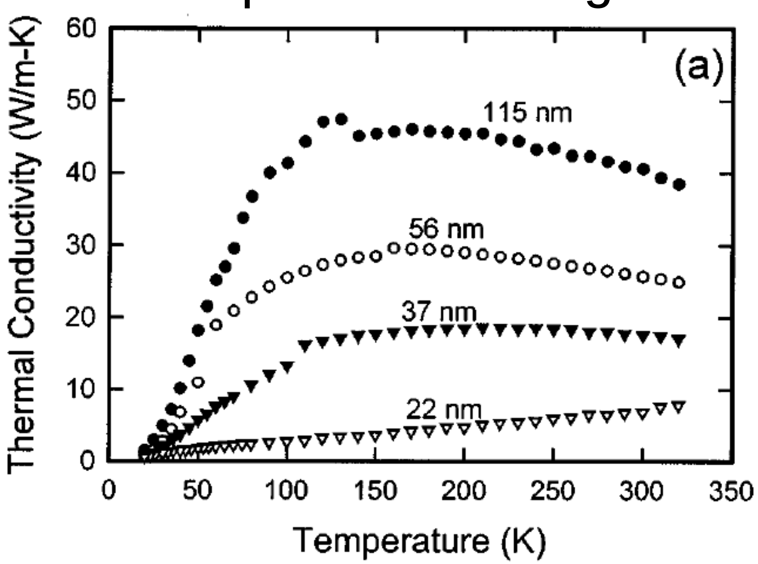

- Si (111) nanowires[1]
- Radius = 11, 18.5, 28, 57.5 nm
- Data: Thermal conductivity
- Predictive challenge: Size effect!

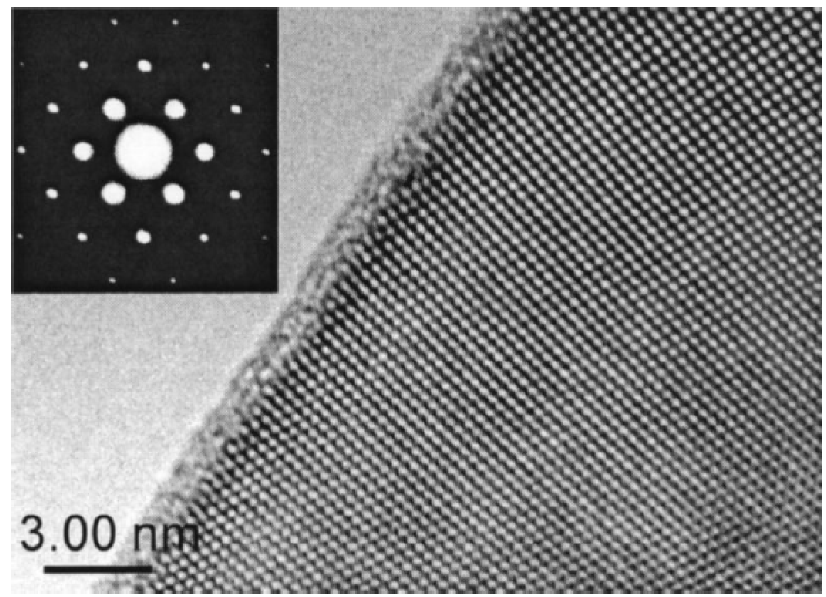

Amorphous layer in SiNW!

[1]D. Li, Y. Yu, P. Kim, L. Shi, P. Yang and A. Majumdar, *Appl. Phys. Let.*,**83** (2003) 2934.

Kinetic validation – Si nanowires

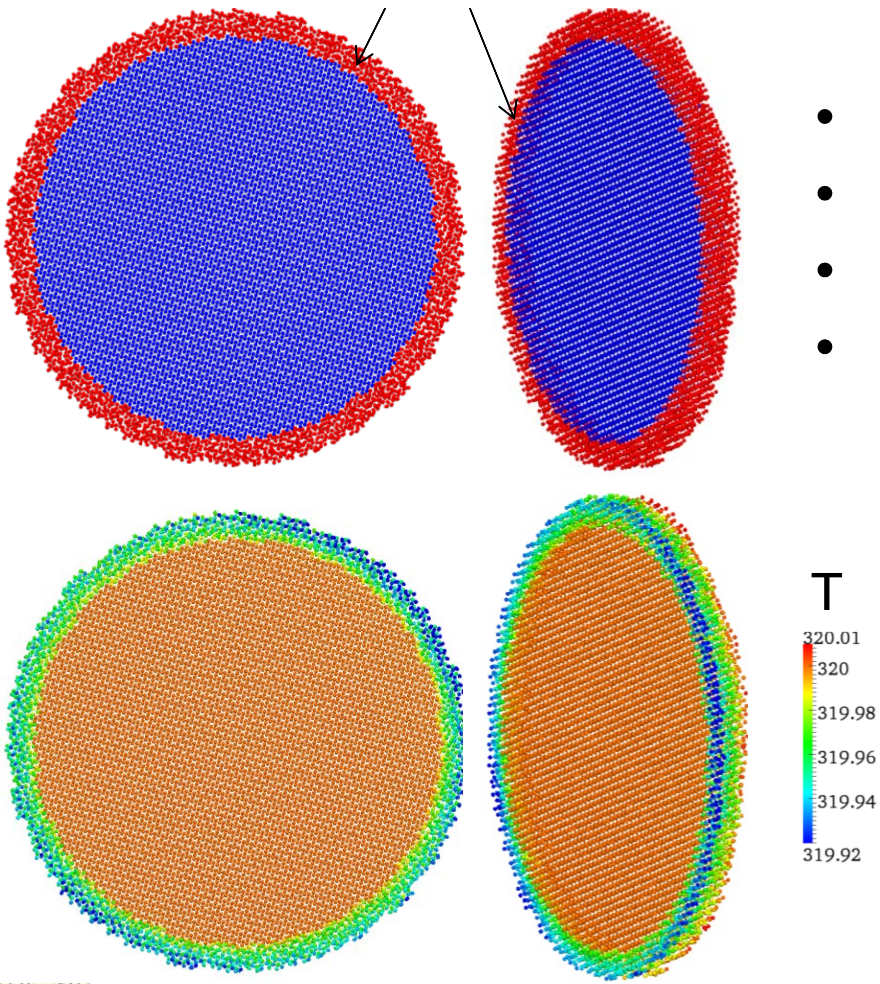

Temperature distribution

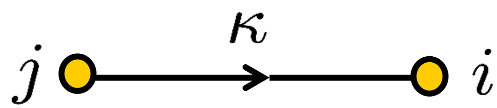

- Rigid model, linear kinetics
- κ_{xal} = 0.09 nW/K, κ_{amo} = 16 nW/K
- Prescribed temperature gradient
- Output: Average axial heat flux

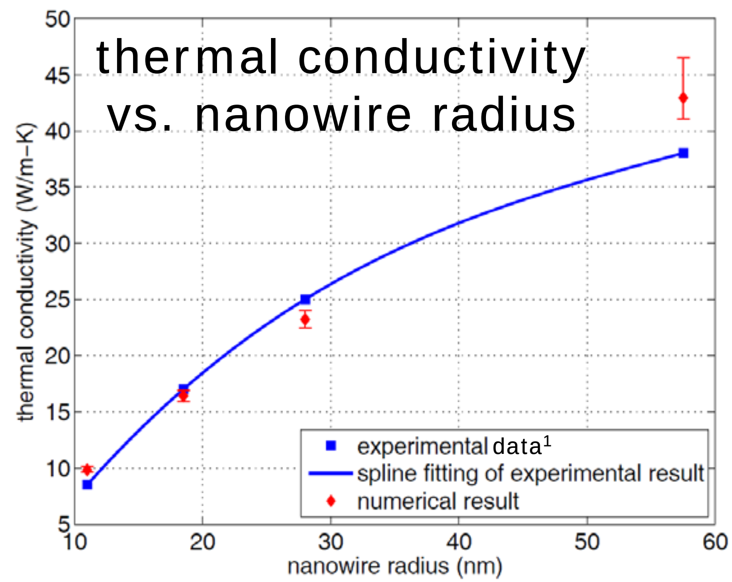

[1]D. Li, Y. Yu, P. Kim, L. Shi, P. Yang and A. Majumdar, *Appl. Phys. Let.*,**83** (2003) 2934.

Kinetic validation – H absorption in Pd

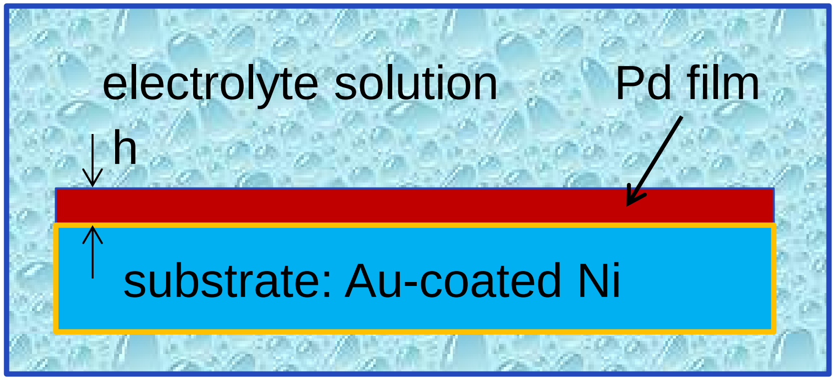

Experimental configuration[1]

- H absorption into (111) Pd foil[1]
- Foil thickness = 460, 1350 Å
- Temperature = 300K
- Measurement: Surface concentration gradient vs. time

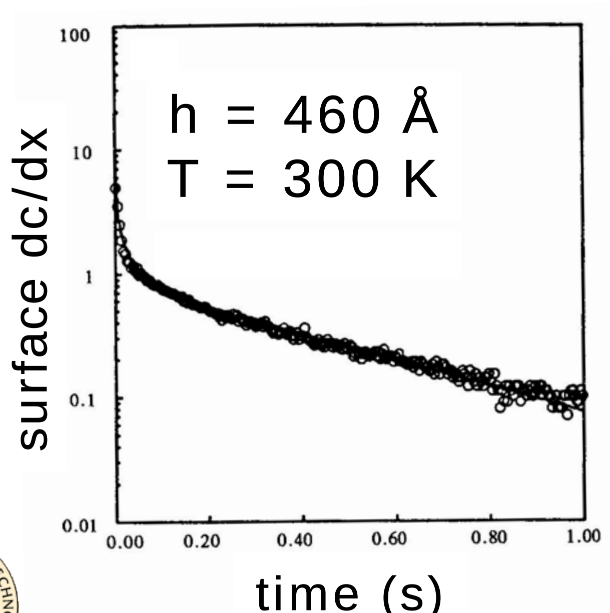

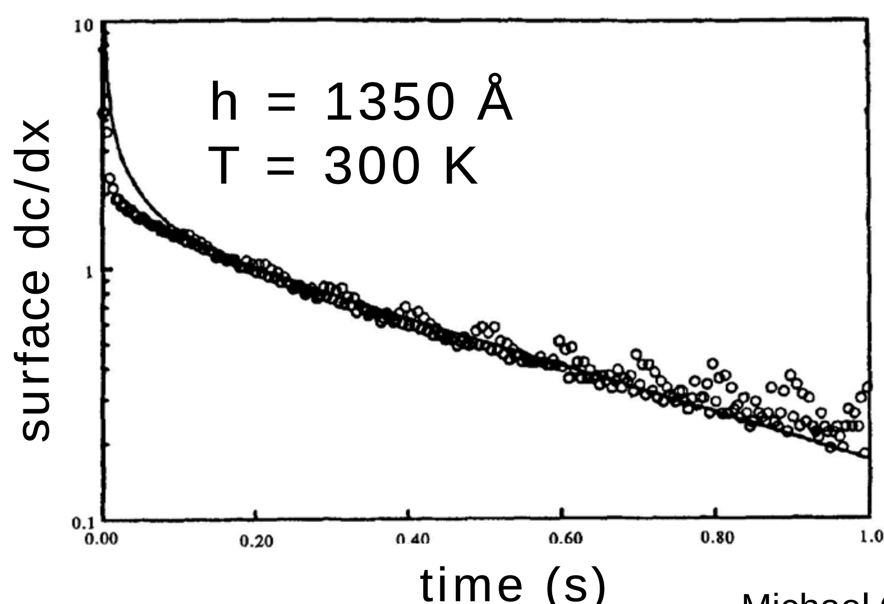

[1]Y. Li and Y.-T. Cheng,, *Int. J. Hydrogen Energy*, **21** (1996) 281-291.

Kinetic validation – H absorption in Pd

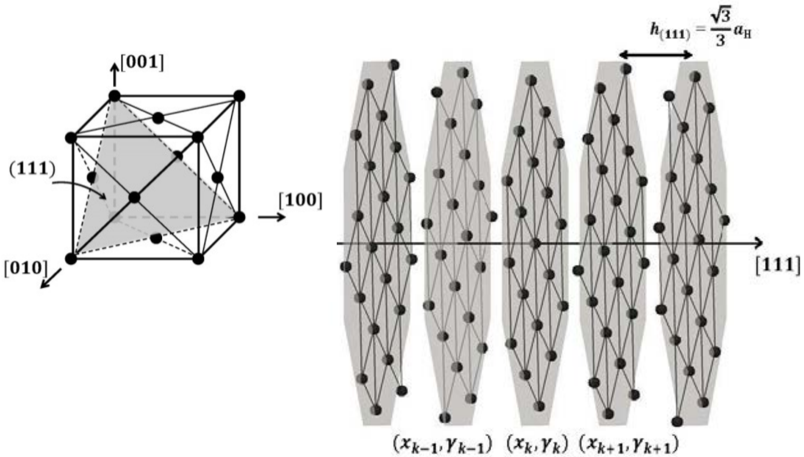

Pd foil crystallography

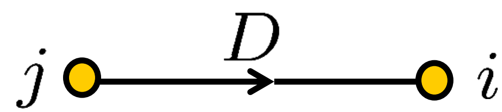

- Linear kinetics, D = 2.1x10^5 Å^2/s
- Ising-type meanfield model
- Johnson EAM potential[1]
- Prescribed surface concentration
- Output: Surface dc/dx vs. time

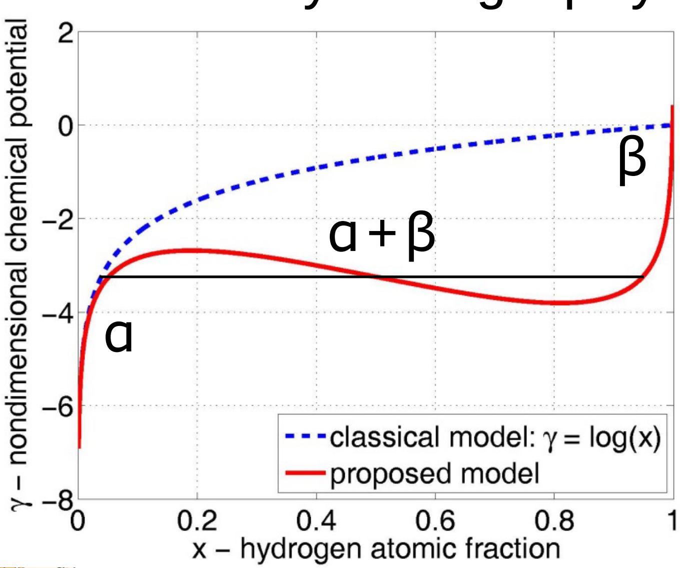

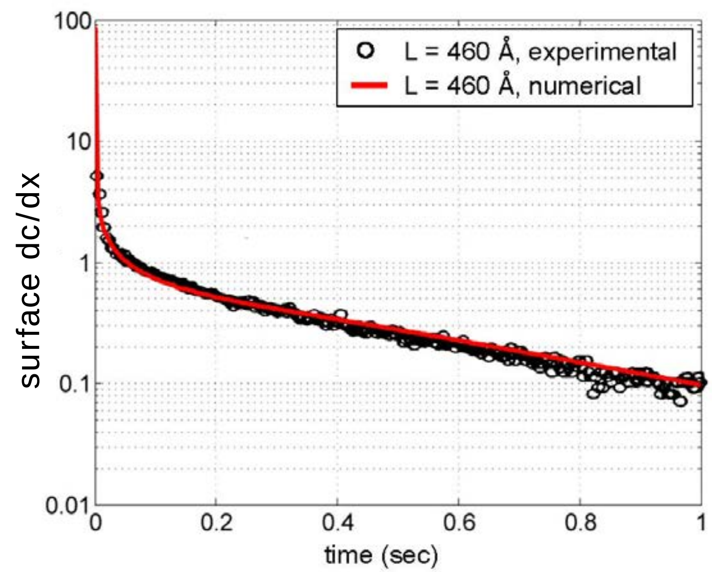

[1]R. Johnson, *Phys. Rev. B*, **39**(17):12554, 1989

[2]Y. Li and Y.-T. Cheng,, *Int. J. Hydrogen Energy*, **21** (1996) 281-291.

Kinetic validation – H absorption in Pd

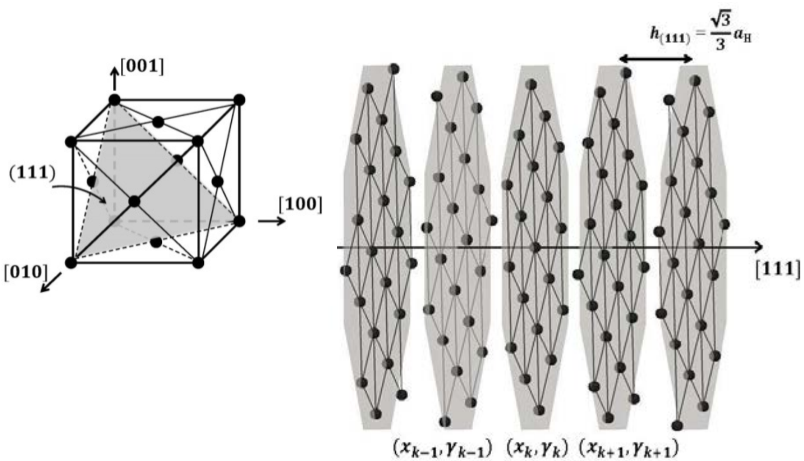

Pd foil crystallography

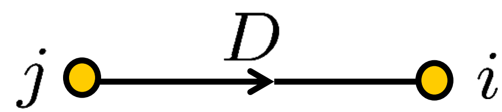

- Linear kinetics, D = 2.1x10^5 Å^2/s
- Ising-type meanfield model
- Johnson EAM potential[1]
- Prescribed surface concentration
- Output: Surface dc/dx vs. time

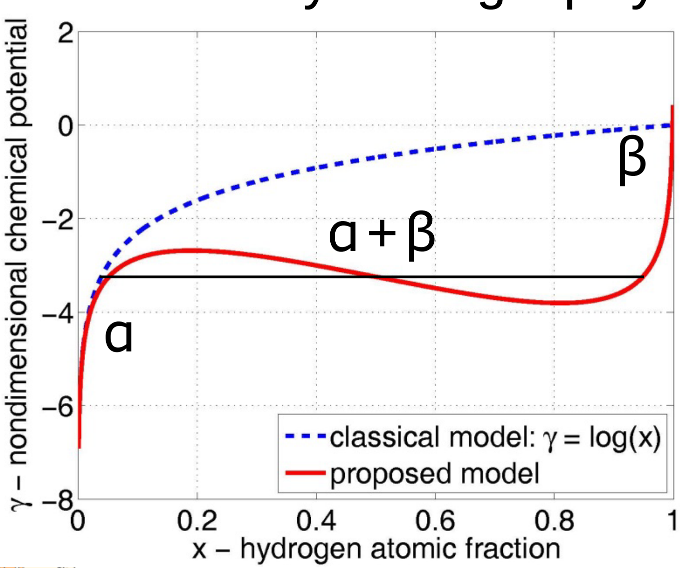

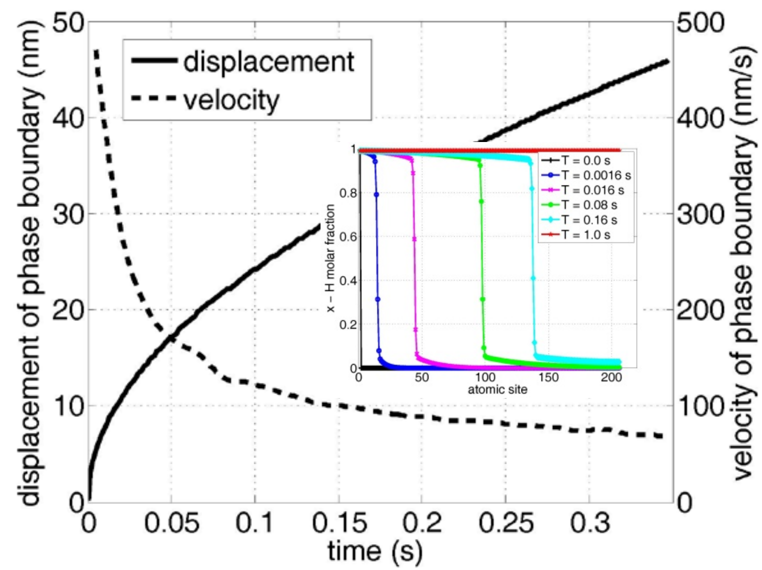

[1]R. Johnson, *Phys. Rev. B*, **39**(17):12554, 1989

[2]Y. Li and Y.-T. Cheng,, *Int. J. Hydrogen Energy*, **21** (1996) 281-291.

Application: Nanovoid cavitation in Cu[1]

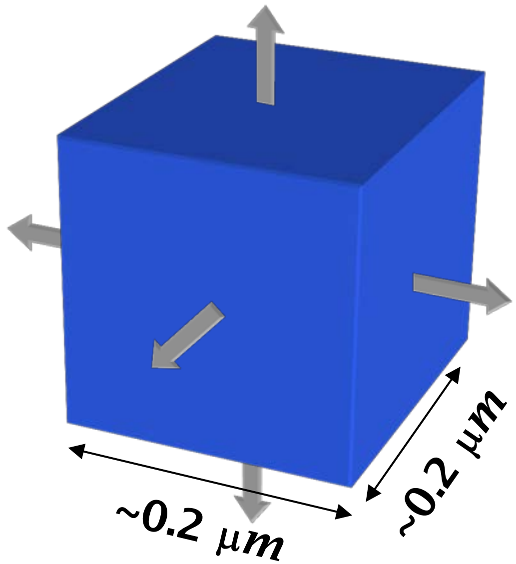

- Parameters:
  - T_0 *(initial) = 300K*
  - *Full Size =* $72a_0$
  - *Atomistic Zone =* $14a_0$
  - *Diameter =* $12a_0$
  - *Strain Rate =* 10^5-10^{12} s^{-1}
- Loading: Triaxial, uniaxial
- Potential: EAM-Mishin[2]

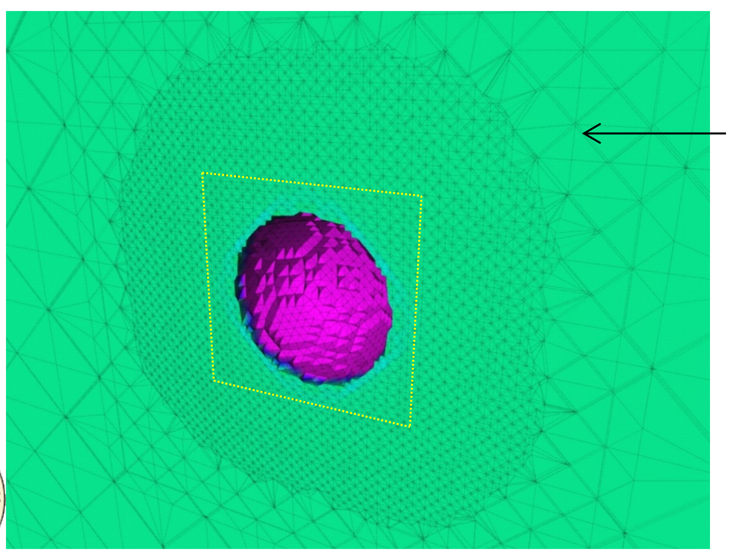

Initial quasicontinuum mesh with full atomistic resolution near void

[1]M. Ponga, M. Ortiz and P. Ariza, *Mechanics of Materials* (submitted)

[2]Y. Mishin, M. Mehl, D. Papaconstantopoulos, A. Voter, A. and J. Kress, *Phys. Rev. B*, **63** (2001) 224106.

Application: Nanovoid cavitation in Cu

Uniaxial loading

Initial Void

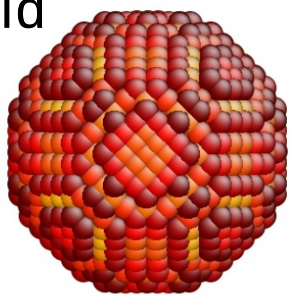

Void at 6.5%

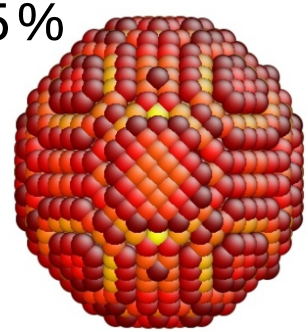

Void at 6.7%

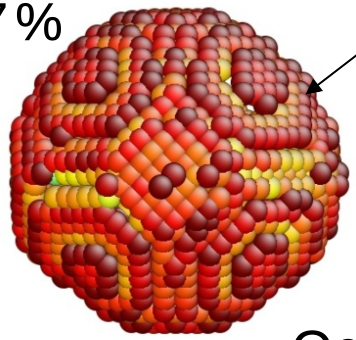

cavitation

Void at 8.5%

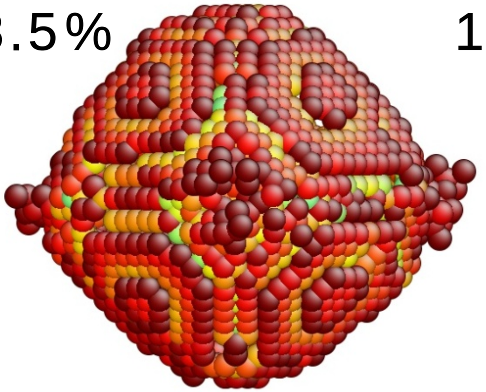

Void at 10.0%

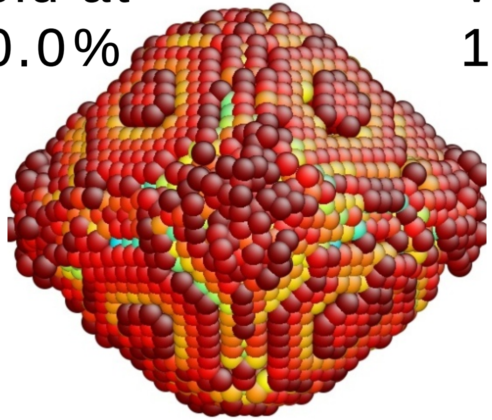

Void at 12.0%

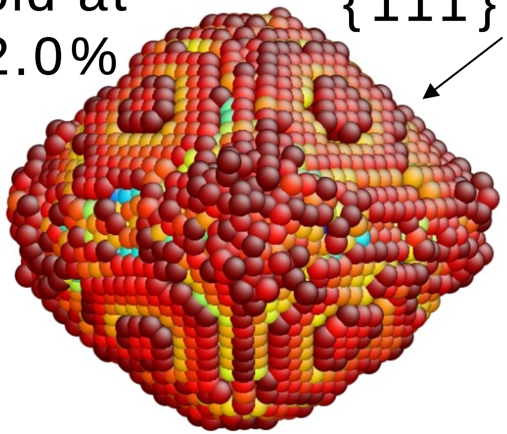

Octahedron {111} planes

Application: Nanovoid cavitation in Cu

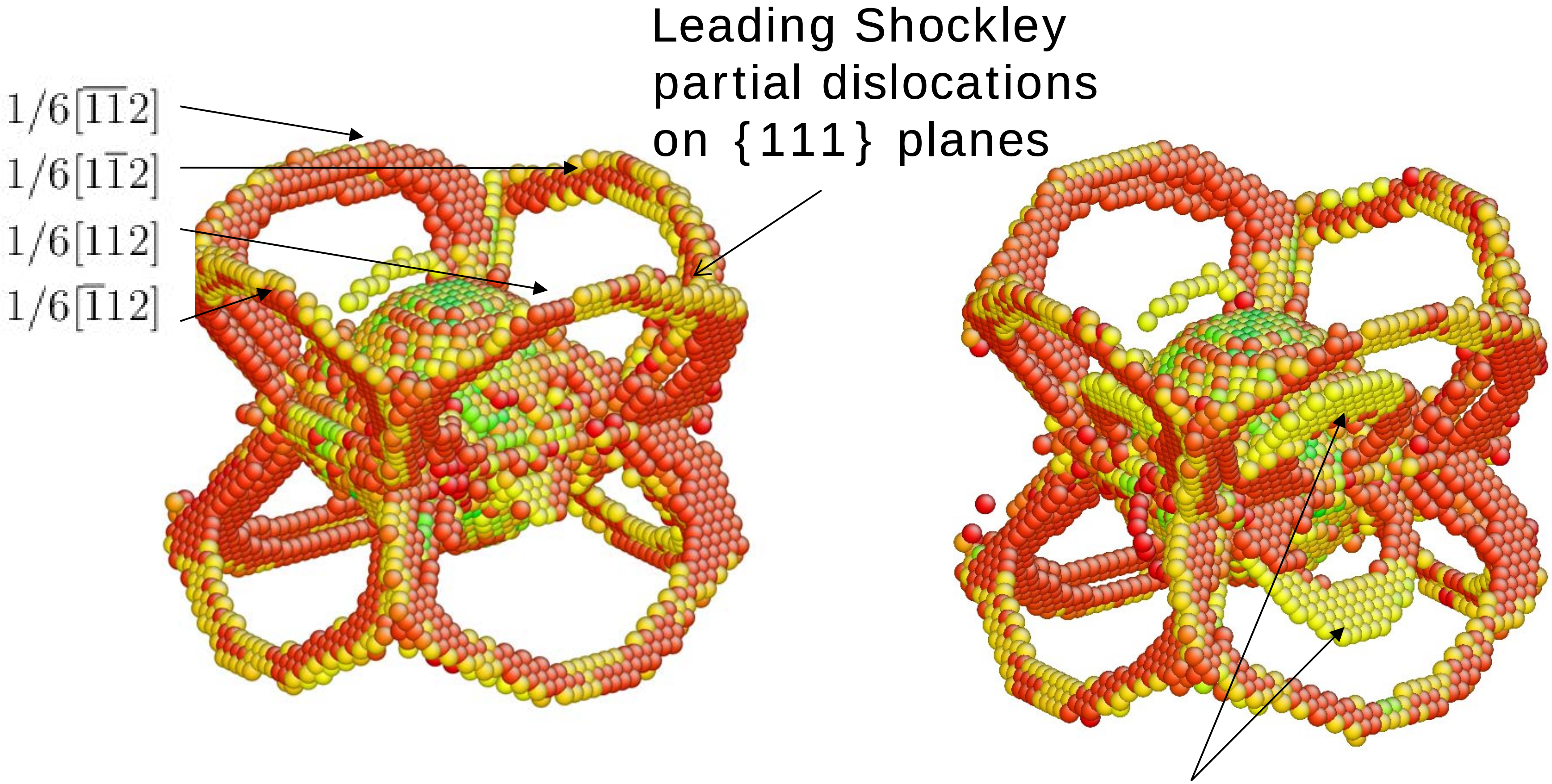

Uniaxial loading, $\varepsilon = 6.6\%$

Application: Nanovoid cavitation in Cu

Shear to Prismatic loop reactions:

On <110> directions

$$1/6[\bar{2}11] + 1/6[\bar{2}1\bar{1}] + 1/6[\bar{1}21] + 1/6[\bar{1}2\bar{1}] \rightarrow [\bar{1}10]$$

$$1/6[\bar{2}\bar{1}\bar{1}] + 1/6[\bar{2}\bar{1}1] + 1/6[\bar{1}\bar{2}\bar{1}] + 1/6[\bar{1}\bar{2}1] \rightarrow [\bar{1}\bar{1}0]$$

$$1/6[1\bar{2}1] + 1/6[1\bar{2}\bar{1}] + 1/6[2\bar{1}1] + 1/6[2\bar{1}\bar{1}] \rightarrow [1\bar{1}0]$$

$$1/6[211] + 1/6[12\bar{1}] + 1/6[21\bar{1}] + 1/6[121] \rightarrow [110]$$

On <110> directions

$$1/6[\bar{2}\bar{1}\bar{1}] + 1/6[\bar{1}\bar{1}\bar{2}] + 1/6[\bar{2}1\bar{1}] + 1/6[\bar{1}1\bar{2}] \rightarrow [\bar{1}0\bar{1}]$$

$$1/6[1\bar{1}\bar{2}] + 1/6[2\bar{1}\bar{1}] + 1/6[21\bar{1}] + 1/6[11\bar{2}] \rightarrow [10\bar{1}]$$

$$1/6[2\bar{1}1] + 1/6[211] + 1/6[1\bar{1}2] + 1/6[112] \rightarrow [101]$$

$$1/6[1\bar{1}2] + 1/6[\bar{2}11] + 1/6[\bar{2}\bar{1}1] + 1/6[\bar{1}\bar{1}2] \rightarrow [\bar{1}01]$$

On <110> directions

$$1/6[\bar{1}21] + 1/6[\bar{1}12] + 1/6[\bar{1}21] + 1/6[112] \rightarrow [011]$$

$$1/6[1\bar{2}\bar{1}] + 1/6[\bar{1}\bar{2}\bar{1}] + 1/6[1\bar{1}\bar{2}] + 1/6[\bar{1}\bar{1}\bar{2}] \rightarrow [0\bar{1}\bar{1}]$$

$$1/6[\bar{1}\bar{2}1] + 1/6[1\bar{2}1] + 1/6[\bar{1}\bar{1}2] + 1/6[1\bar{1}2] \rightarrow [0\bar{1}1]$$

$$1/6[1\bar{2}1] + 1/6[11\bar{2}] + 1/6[\bar{1}1\bar{2}] + 1/6[12\bar{1}] \rightarrow [01\bar{1}]$$

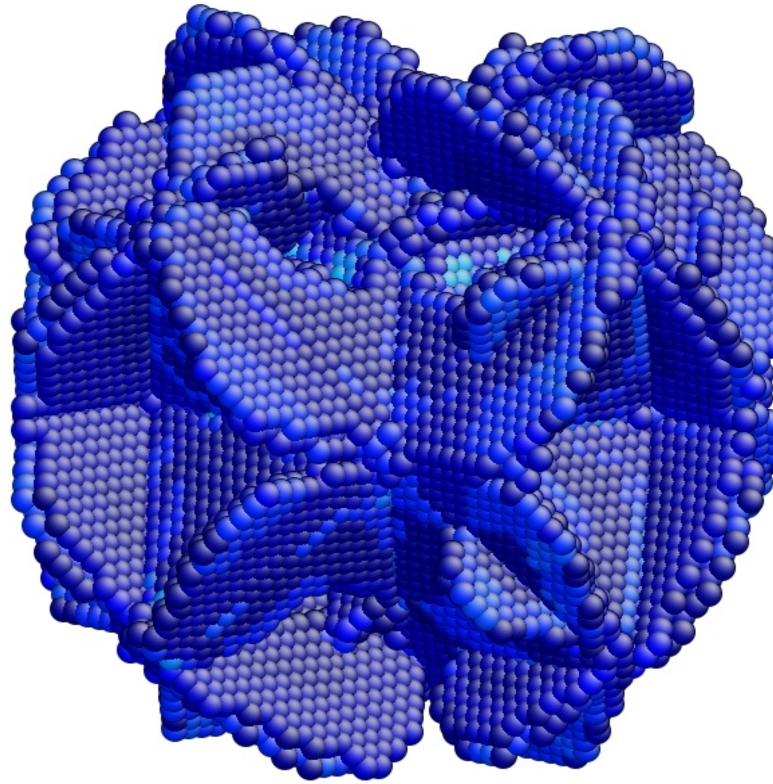

Triaxial loading

Application: Nanovoid cavitation in Cu

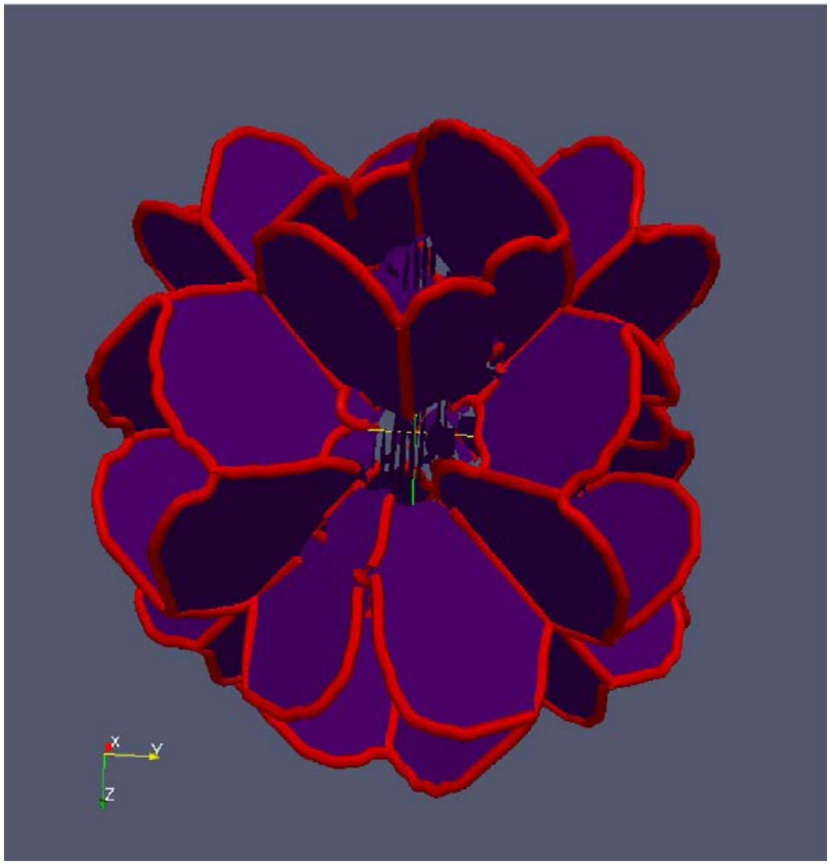

Prismatic loop structure, triaxial loading

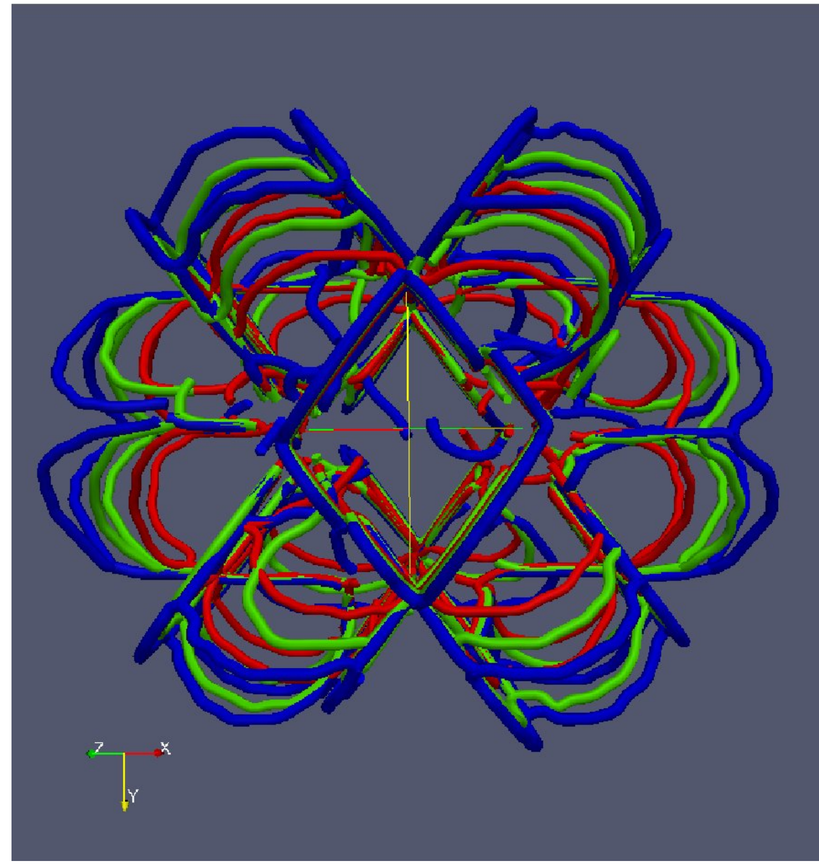

Prismatic loop evolution (ε = 5, 6, 7%)

(Images obtained with **DXA** and **Paraview**)

Application: Nanovoid cavitation in Cu

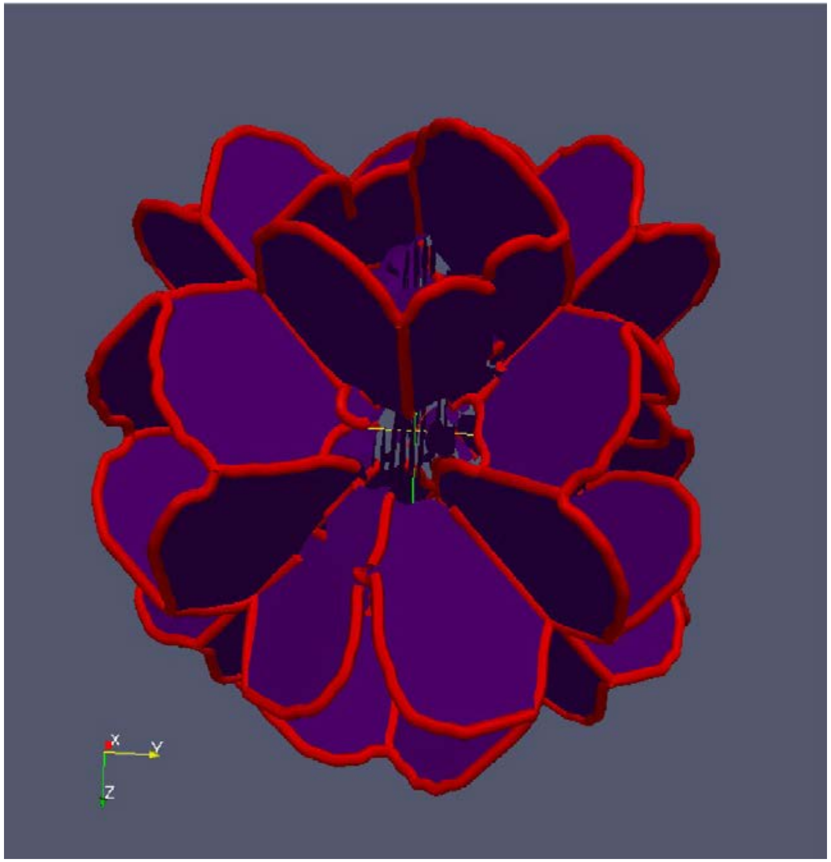

Prismatic loop structure, triaxial loading

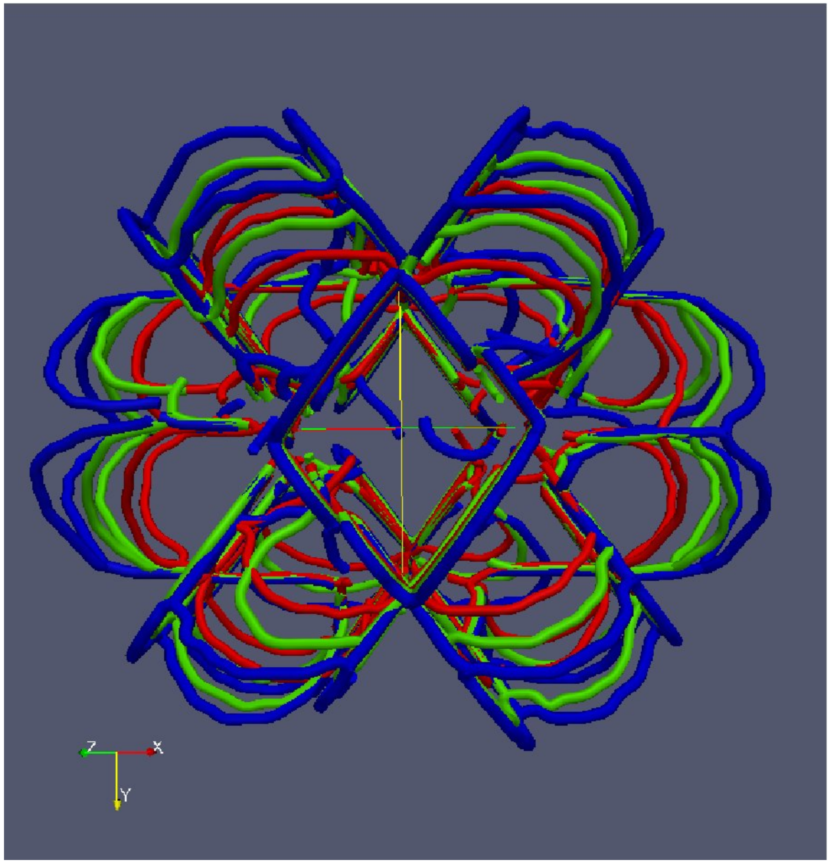

Prismatic loop evolution (ε = 5, 6, 7%)

(Images obtained with **DXA** and **Paraview**)

Application: Nanovoid cavitation in Cu

Temperature increase on {111} planes due to dislocation activity

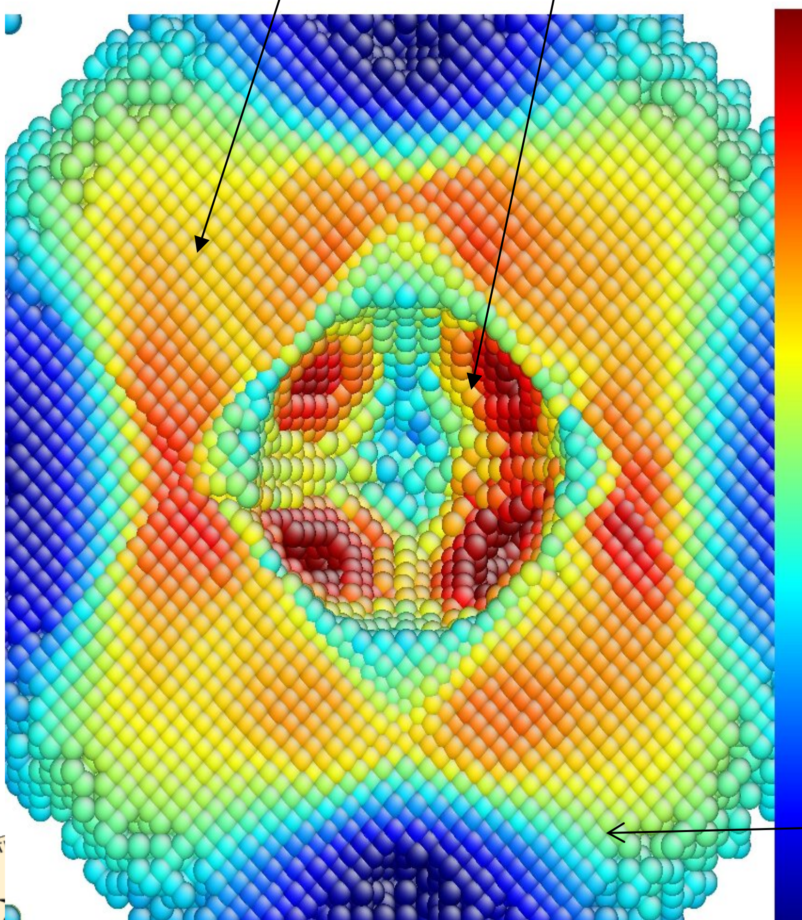

Temperature evolution

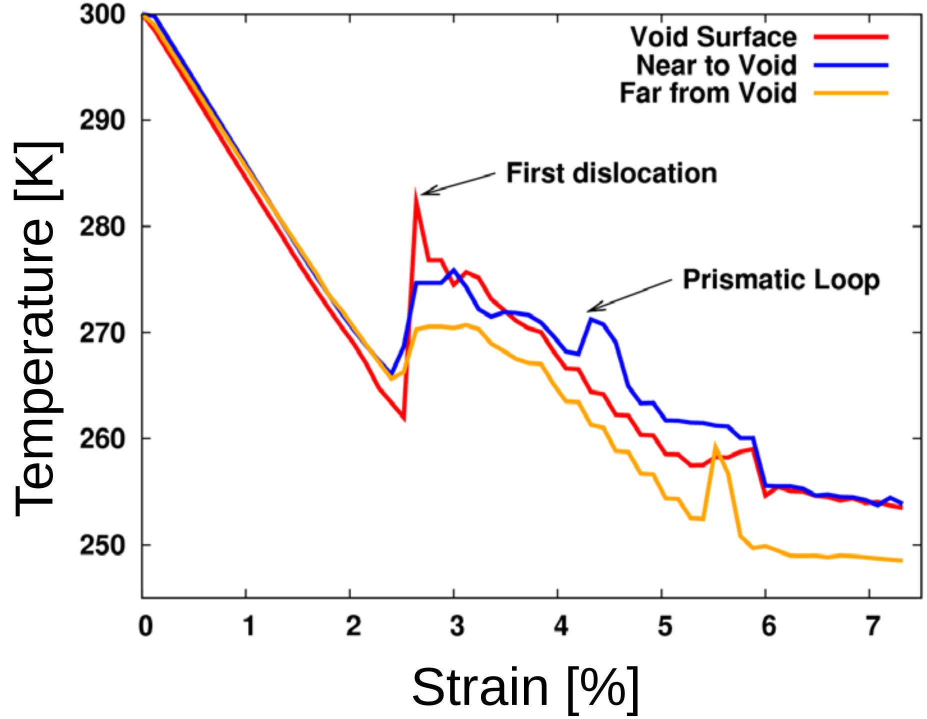

Temperature field @ ε=2.7%

Michael Ortiz
PIRE 09/14

Application: Nanovoid cavitation in Cu

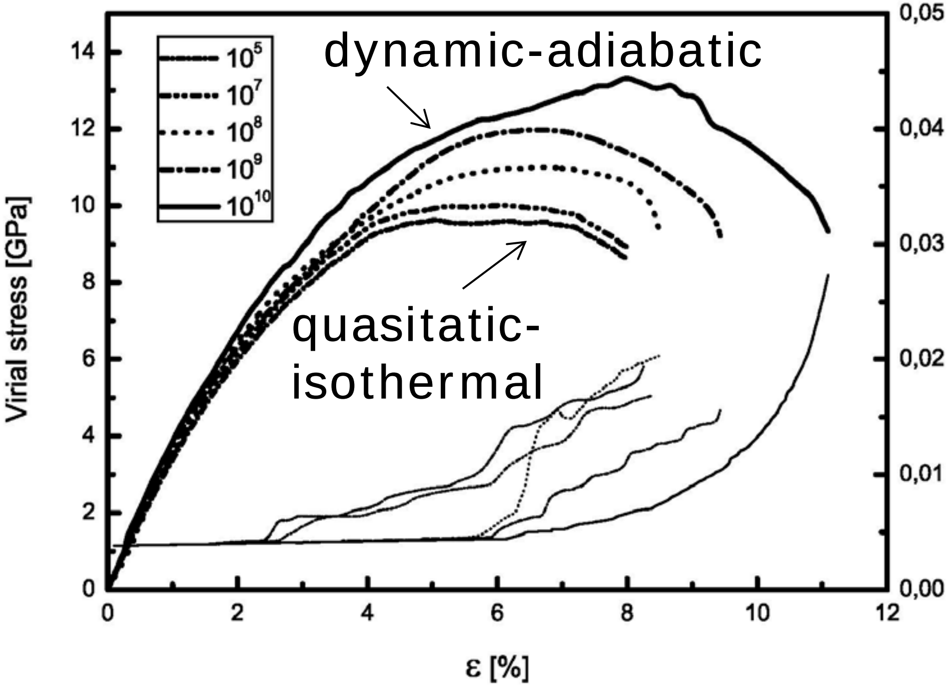

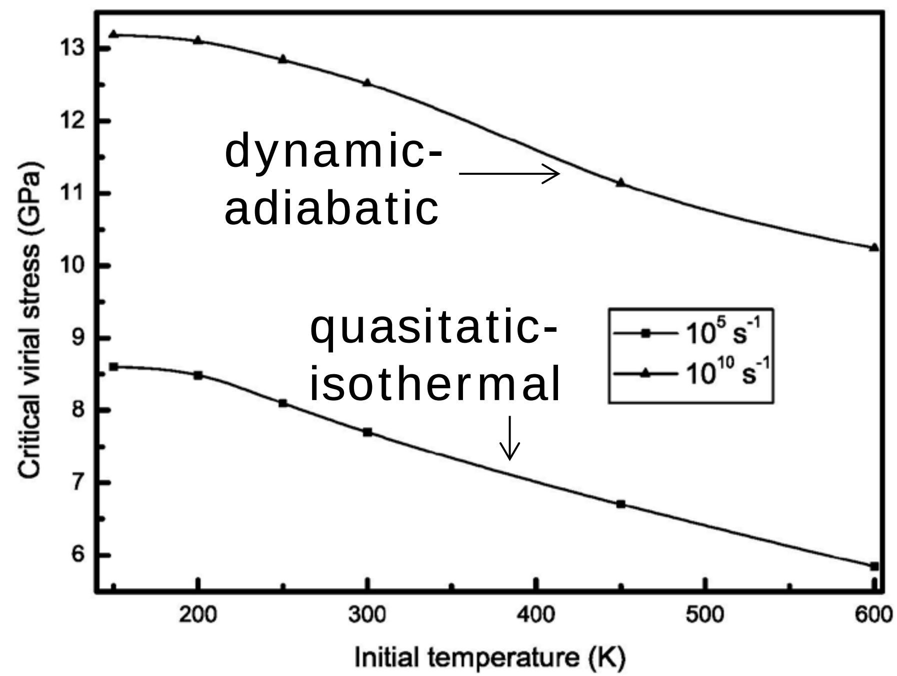

- Transition between quasistatic-isothermal to dynamic-adiabatic behavior at 10^7-10^8 s^{-1}
- Quasistatic regime: Time scale set by heat conduction
- Dynamic regime: Time scale set by microinertia

Spacetime atomistic-to-continuum

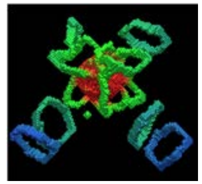

Tang, Y. *et al*., *Acta Mater.*, **59**:1354, 2011.

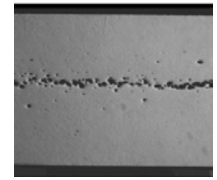

R. Becker, *S&T. Rev.*, (LLNL) July/Aug 2002

Paradigm	Atomistic	Mesoscopic
Configuration space	Phase space (micro)	•Phase space (meso) •Temperature •Concentrations
Governing equations (axioms, postulates)	ΣF=ma (micro)	•ΣF=ma (meso) •Diffusive transport
Spatial resolution	Atomic lattice	•Atomic near defects •Continuum elsewhere
Temporal resolution	•Thermal vibrations •Transition states	•Elastic waves (meso) •Diffusional transients
Input to the model	Empirical interatomic potentials	•Empirical potentials •Empirical kinetics

Concluding remarks

- Many applications require both atomistic input and the computation of *long term behavior*
- We need spatial and *temporal coarse-graining*!
- *Non-equilibrium statistical* mechanics allows thermal fluctuations and atomic hops to be treated *statistically*
- It defines a *mesoscopic dynamics* that is coupled to heat and mass transport equations from atomistic input (*empirical* interatomic potentials and *transport kinetic potentials*)
- A more rigorous derivation from fundamental theory strongly to be desired...